Electronic Supplementary Material (ESI) for New Journal of Chemistry.

Supporting Information

Facile synthesis of O-doped carbon nitride nanofibers for two-step single-electron oxygen reduction to H_2O_2

Tingshuo Ji,[a] Xue Wei,[a] Juanjuan Wang,[a] Yuanjing Fan,[a] Ziwei Wang,[a] Shengxian Zhou,[a] Xuefeng Wei*[b], Baocheng Yang*[a] and Yanzhen Guo*[a]

[a]Henan Provincial Key Laboratory of Nanocomposites and Applications, Institute of Nanostructured Functional Materials, Huanghe Science and Technology College, Zhengzhou 450006, China. E-mail: baochengyang@infm.hhstu.edu.cn; yzguo@hhstu.edu.cn

[b]College of Chemical Engineering & Pharmaceutics, Henan University of Science and Technology, Luoyang, 471023, PR China. E-mail: xfwei@haust.edu.cn

1. Experimental details

1.1. Preparation of the photocatalysts

The CNF photocatalyst was synthesized according to a previous report with slight modification.[S1] Typically, cyanuric chloride (4.0 mmol) and melamine (2.0 mmol) were successively added into 30 mL of acetonitrile, followed by ultrasonic dispersion. Then the mixture was stirring for 24 h at 25°C, and solvothermally reacted for 24 at 180°C. The precipitate was then collected and centrifuged several times with ultrapure water and anhydrous ethanol to remove impurities on the surface. The product was then dried in a 60°C oven.

The O-doped g-C_3N_4 samples were synthesized through one-pot solvothermal method with addition of the representative amino acid. Cyanuric chloride (4.0 mmol) and melamine (2.0 mmol) were first dissolved in 30 mL of acetonitrile Then a certain amount of amino acid (L-arginine, L-cysteine or L-lysine) was added into the above mixture. The O-doped g-C_3N_4 samples of ACN*x*, CCN*x* or LCN*x* were respectively acquired with the same solvothermal procedure with that of CNF. In the abbreviations of ACN*x*, CCN*x* and LCN*x*, *x* denotes the addition amount (mmol) of the amino acids. Especially, ACN, CCN, and LCN are abbreviated for ACN0.1, CCN0.1, and LCN0.1.

1.2 Characterizations

The morphologies of the catalysts were observed on scanning electron microscope (SEM, Quanta 250 FEG FEI) and transmission electron microscope (TEM) (Tecnai G2 20

TEM). The light harvesting capacities of the samples were characterized by their absorption spectra on a Hitachi ultraviolet/visible/near-infrared (UV-vis-NIR) spectrophotometer equipped with an integrating sphere with $BaSO_4$ as a base. The crystalline characteristics of the samples were investigated by collecting their X-ray diffraction (XRD) patterns on a Bruker D8 Advance diffractometer with tube voltage and current of 40 kV and 40 mA, respectively. The Fourier transform infrared (FTIR) spectra of the samples were collected on a Thermo Scientific Nicolet iS5 infrared spectrophotometer using potassium bromide pellet technique. X-ray photoelectron spectroscopy (XPS) measurements were recorded on an Escalab 250 Xi (Thermo Fisher Scientific) system with Al Kα ($h\upsilon$ = 1486.6 eV) as the X-ray source. The photoluminescence (PL) measurements (Hitachi F-4600 spectrophotometer) were carried out to investigate the radiative recombination of the photogenerated charge carriers. The transient-state photoluminescence (TRPL) spectra were recorded on Edinburgh Instruments FLS980 spectrophotometer with excitation and emission wavelength of 350 and 455 nm, respectively. N_2 adsorption-desorption isotherms, which were used to calculate the Brunauer-Emmett-Teller (BET) specific surface areas, were collected on a Micromeritics ASAP 2020 analyzer. The Solid-state ^{13}C nuclear magnetic resonance (NMR) was performed on JNM-ECZ600R nuclear magnetic resonance spectrometer. The thermogravimetric analysis was carried out on a thermogravimetric-differential scanning calorimetry analyzer (SDT Q600). O_2-temperature programmed desorption (O_2-TPD) was performed on a chemisorption instrument (TP-5080). Electron paramagnetic resonance (EPR) spectra of the samples

were collected on a Brucker EMXnano spectrometer with 5,5-dimethyl-1-pyrroline N-oxide (DMPO) as the trapping agents of $\bullet O_2^-$.

1.3 Photocatalytic performance measurements

The photocatalytic performances of the photocatalysts were evaluated through the photogeneration of H_2O_2 in a photoreactor by employing a 300 W Xe lamp (CEL-HXF300, CEAULIGHT, Beijing, China) equipped with a cut-off filter of 420 nm as the light source. Typically, the photocatalyst (50 mg) was first dispersed into an ethanol aqueous solution (50 mL, 10 vol% ethanol in deionized water) and sonicated for 5 min to ensure the uniformity of the suspension. Then the mixture was bubbled with O_2 for 20 min to create an oxygen-rich environment before light was turned on. During photocatalytic process, every 1.5 ml of solution was taken out from the reaction mixture with time interval of 0.5 h. The concentration of H_2O_2 generated in the reaction solution was determined by a $Ce(SO_4)_2$ titration method with the assistance of UV-vis spectrophotometer. Moreover, the evolution amount of H_2O_2 under monochromatic light was measured by replacing the cut-off filter with a bandpass filter. The power intensity of monochromatic light was measured with an optical power meter (CEL-NP2000-2, CEAULIGHT, Beijing, China). The apparent quantum yield (AQY) was estimated by the H_2O_2 amount generated under monochromatic light and corresponding power density according to the equation: AQY (%) = (number of reacted electrons/number of incident photons) × 100 = (2×number of produced H_2O_2 molecules)/(number of incident photons) × 100.

1.4. Photoelectrochemical measurements

The photoelectrochemical measurements were carried out on a CHI 760E electrochemical workstation (Shanghai Chenghua) by using a standard three-electrode system, in which the sample electrode, the Ag/AgCl electrode and the Pt plate electrode were served as the working electrode, the reference electrode and the counter electrode, respectively. The sample electrode was prepared by depositing photocatalyst suspension (10 mg/mL in 5.0 vol% Nafion ethanol solution) on a cleaned fluorine-doped tin oxide (FTO) glass substrate with a surface area of 1 × 1 cm^2. The aqueous Na_2SO_4 solution (0.5 M) was used as electrolyte.[S2] The normal hydrogen electrode (NHE at pH = 7) can be converted from the reference electrode potential (vs. Ag/AgCl) according to $E_{NHE} = E_{Ag/AgCl} + E^0_{Ag/AgCl}$, where $E^0_{Ag/AgCl}$ is 0.197 V at 25 ^oC.[S3] The Mott-Schottky curves for flat potential confirmation were measured by impedance-potential method. The photocurrent curves were collected at a potential of 0.2 V (vs. Ag/AgCl) under on-off visible light irradiation. The electrochemical impedance spectroscopy (EIS) tests were performed in the frequency range of 0.01 Hz to 100 kHz.

1.5. Rotating ring-disk electrode (RRDE) measurement

RRDE was employed to measure the electron transfer number and H_2O_2 selectivity of CNF and CCN in oxygen reduction process. The electrochemical measurement was carried out in a three-electrode system, in which RRDE, Ag/AgCl and Pt/C were the working, reference and counter electrode. O_2-saturated 0.1 M KOH solution was used

as the electrolyte. The catalyst ink on the RRDE working electrode was prepared by dispersing the photocatalyst into an ethanol solution with 5 vol% nafion (10 mg/mL).

The electron transfer number is calculated according to the following formula: [S4,S5]

$$n=(4\times|I_d|)/(|I_d|+I_r/N)$$

The H_2O_2 selectivity is calculated according to the following formula:

$$H_2O_2(\%)=(200\times I_r/N)/(|I_d|+I_r/N)$$

Where I_r is the ring current, I_d is the disc current, and N is the collection efficiency (N=0.37).

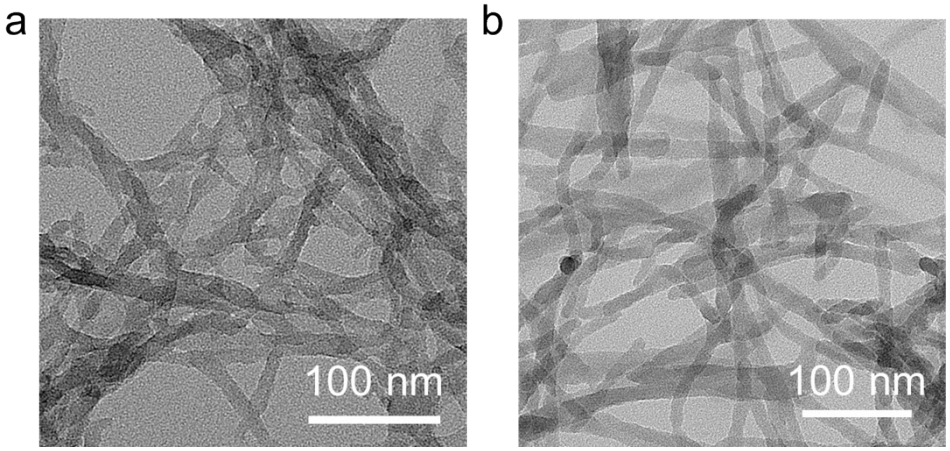

Fig. S1 TEM images of CNF (a), and CCN (b).

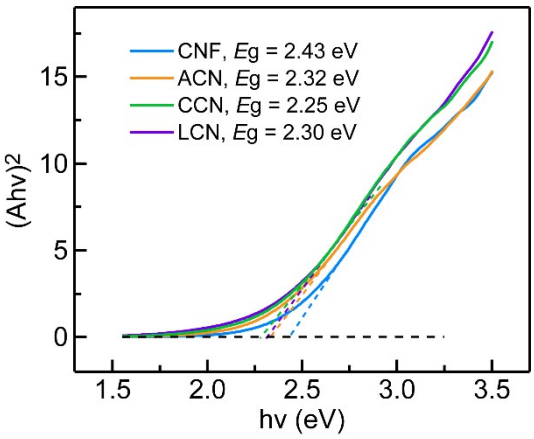

Fig. S2 Tauc plots of the four samples.

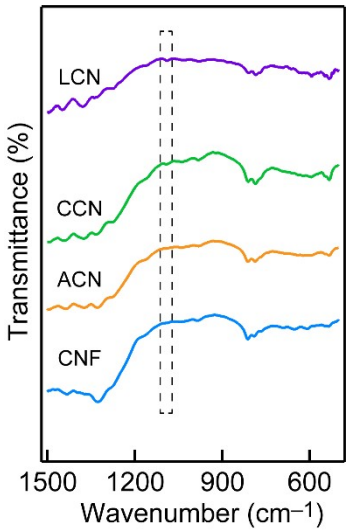

Fig. S3 Enlarged FTIR spectra of the four samples.

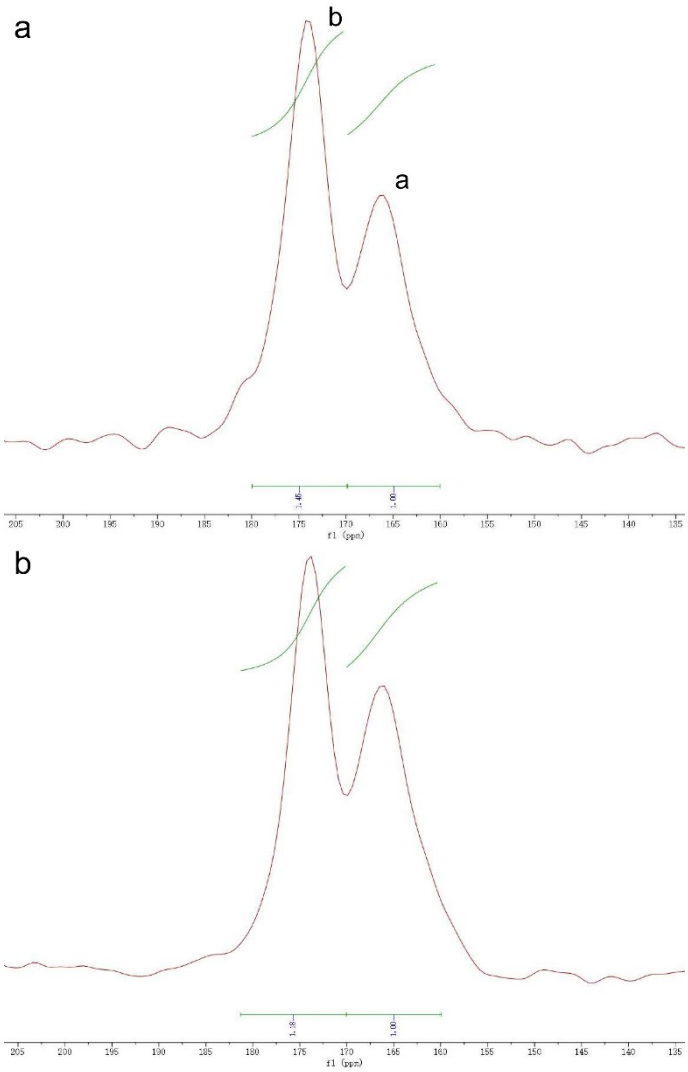

Fig. S4 ^{13}C NMR spectra of CNF (a) and CCN (b).

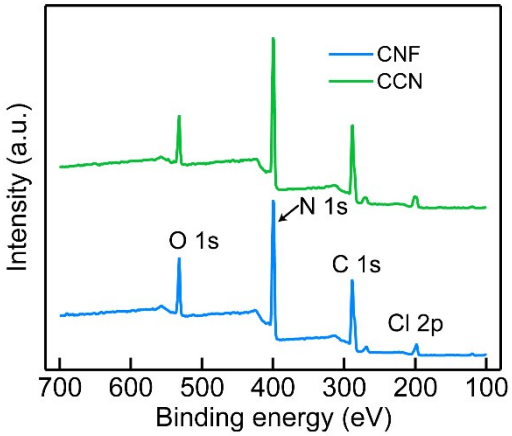

Fig. S5 The survey XPS spectra of CNF and CCN.

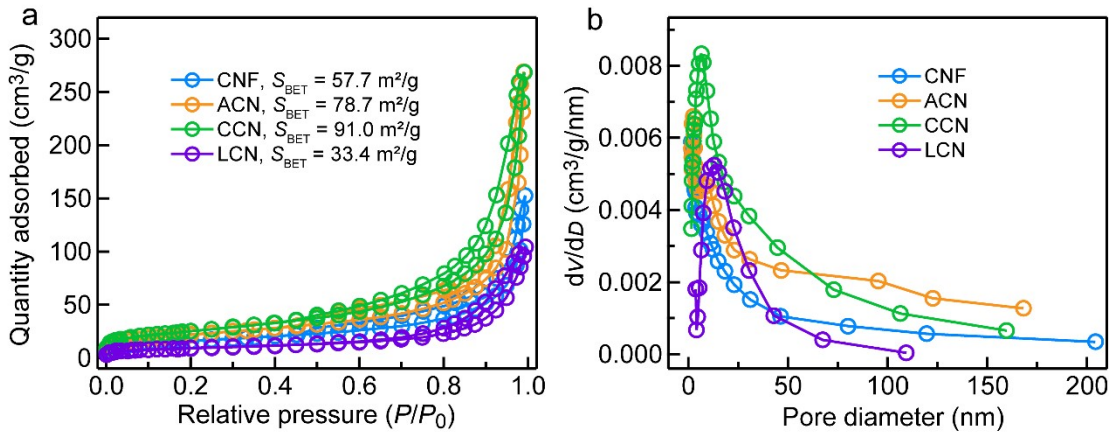

Fig. S6 N_2 adsorption-desorption isotherms (a) and pore structure characterization (b) of the samples.

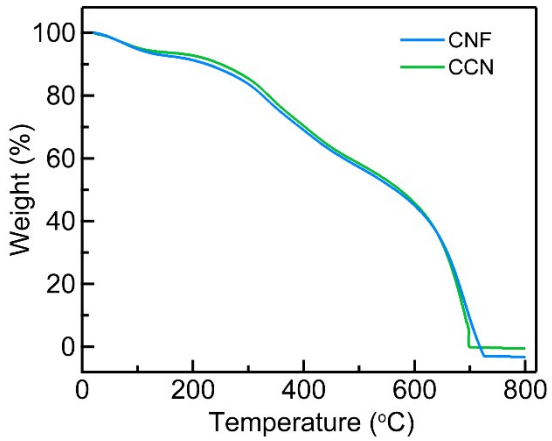

Fig. S7 Thermogravimetric analysis curves of CNF and CCN.

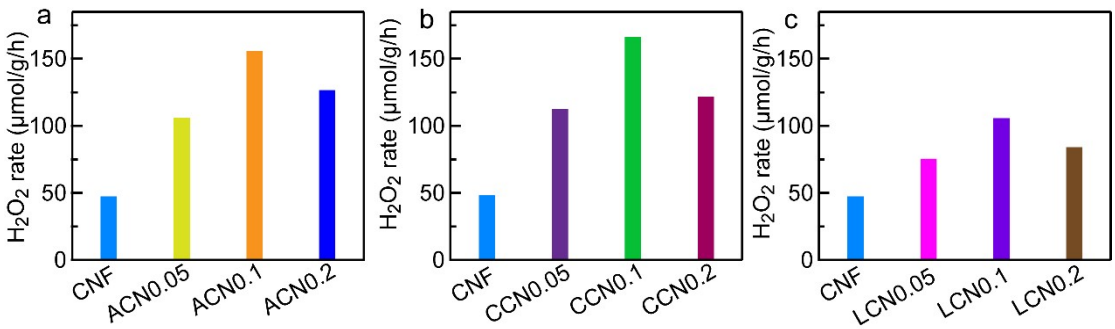

Fig. S8 The photocatalytic H_2O_2 generation activity of ACN*x* (a), CCN*x* (b), and LCN*x* (c).

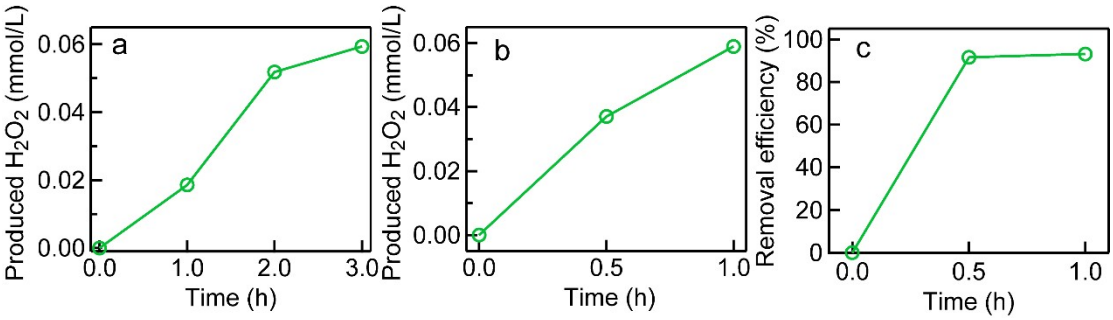

Fig. S9 The photocatalytic H_2O_2 generation reaction with different oxidation reactions. (a) Photocatalytic H_2O_2 generation proceeded in pure water. (b) Photocatalytic H_2O_2 generation proceeded in MB solution. (c) MB removal efficiency during H_2O_2 generation process.

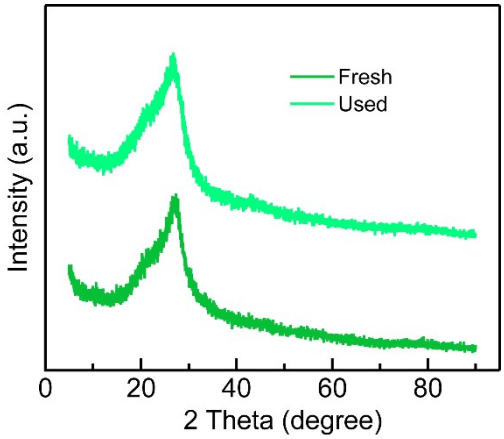

Fig. S10 XRD patterns of the fresh and used CCN sample.

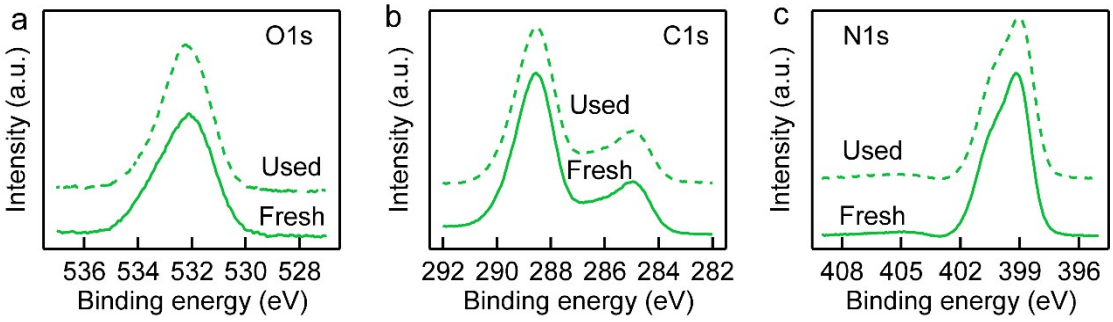

Fig. S11 High-resolution O1s (a), C1s (b) and N1s (c) spectra of the fresh and used CCN sample.

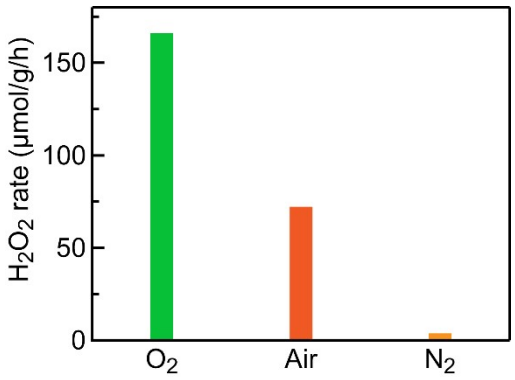

Fig. S12 The photocatalytic H_2O_2 generation of CCN measured under different atmosphere.

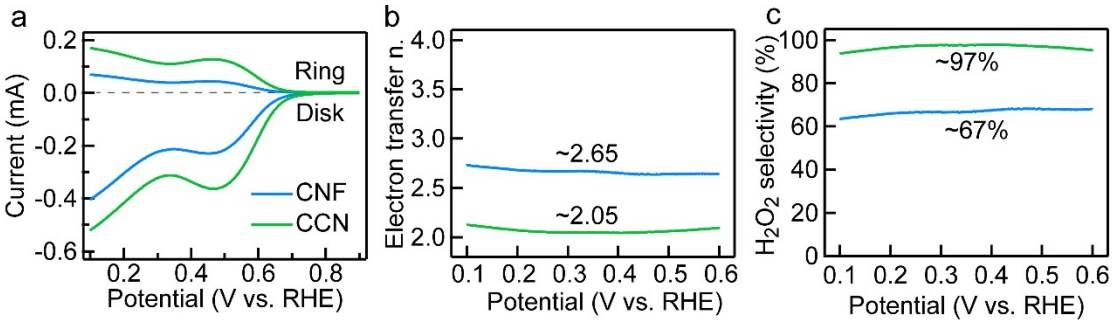

Fig. S13 RRDE measurements of CNF and CCN. (a) RRDE polarization curves in O_2-saturated 0.1 M KOH solution. (b) Electron transfer number and (c) H_2O_2 selectivity calculated from the polarization curves.

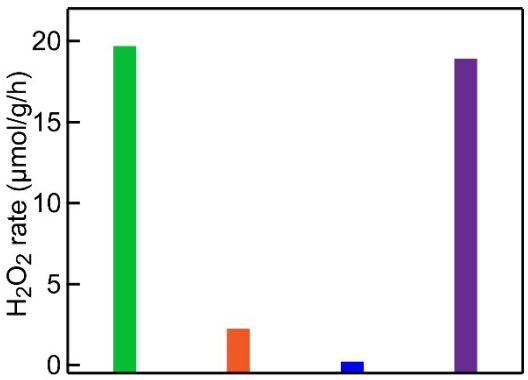

Fig. S14 The photocatalytic H_2O_2 generation rate of CCN in the presence of different

trapping agents.

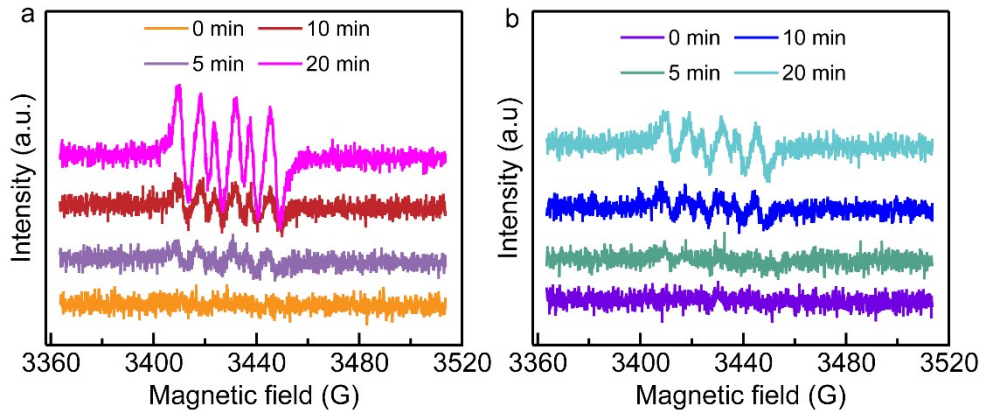

Fig. S15 Detection of $\cdot O_2^-$ over the ACN (a) and LCN (b) samples with different illumination time.

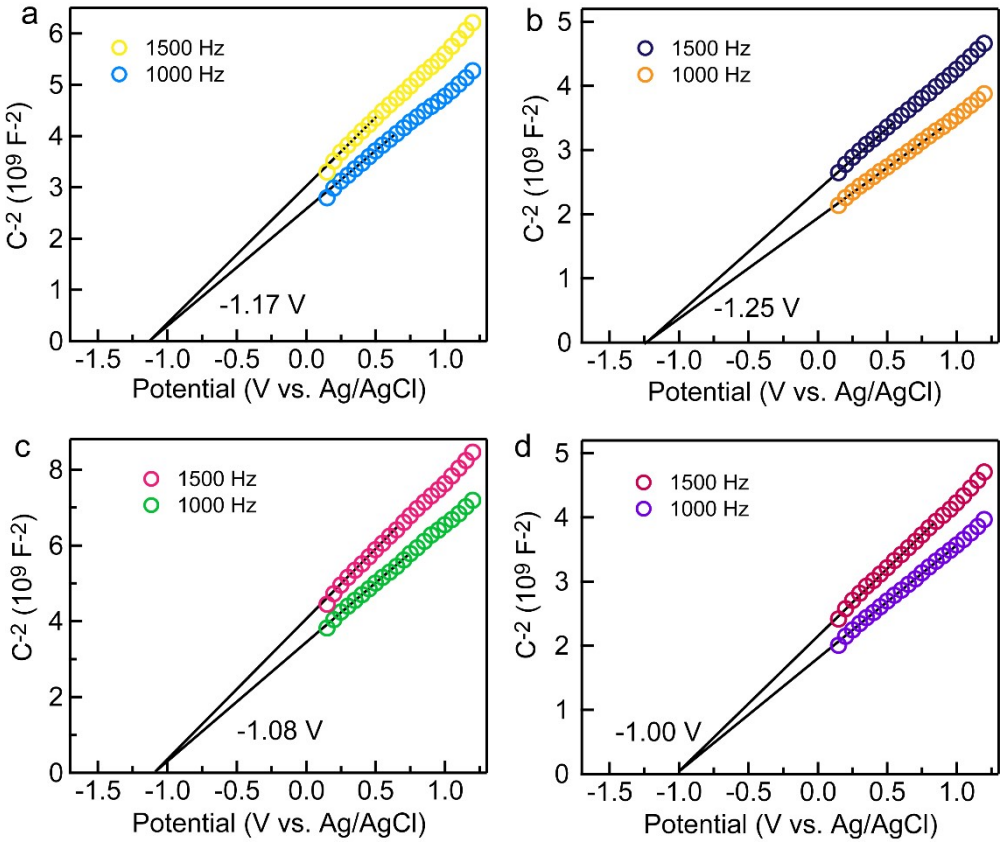

Fig. S16 Mott-Schottky curves of CNF (a), ACN (b), CCN (c), and LCN (d).

References

(S1) Y. J. Cui, Z. X. Ding, X. Z. Fu and X. C. Wang, *Angew. Chem., Int. Ed.*, 2012, **51**, 11814–11818.

(S2) S. J. Hong, S. Lee, J. S. Jang, and J. S. Lee, *Energy Environ. Sci.*, 2011, **4**, 1781–1787.

(S3) W. J. Li, P. M. Da, Y. Y. Zhang, Y. C. Wang, X. Lin, X. G. Gong, and G. F. Zheng, *ACS Nano*, 2014, **8**, 11770–11777.

(S4) C. J. Li, Q. Z. Zheng, Q. Xiang, L. Yu, P. Chen, D. M. Gao, Q. S. Liu, F. L. He, D. M. Yu, Y. P. Liu, C. G. Chen, *J. Chem. Educ.*, 2021, **98**, 3026–3031.

(S5) X. Zhang, P. J. Ma, C. Wang, L. Y. Gan, X. J. Chen, P. Zhang, Y. Wang, H. Li, L. H. Wang, X. Y. Zhou, K. Zheng, *Energy Environ. Sci.*, 2022, **15**, 830.